Antiperovskite active materials for metal-ion batteries

Expected advantages, limitations, and perspectives

Dai, Tian; Kouoi, Xavier; Reynaud, Marine; Wagemaker, Marnix; Valldor, Martin; Famprikis, Theodosios; Koposov, Alexey Y.

DOI
10.1016/j.ensm.2024.103363

Publication date
2024

Document Version
Final published version

Published in
Energy Storage Materials

Energy Storage Materials 68 (2024) 103363

Contents lists available at ScienceDirect

Energy Storage Materials

journal homepage: www.elsevier.com/locate/ensm

Antiperovskite active materials for metal-ion batteries: Expected advantages, limitations, and perspectives

Tian Dai [a,*], Xavier Kouoi [b,c,d], Marine Reynaud [c,d], Marnix Wagemaker [b], Martin Valldor [a], Theodosios Famprikis [b,d,*], Alexey Y. Koposov [a,d,e,*]

[a] Centre for Material Science and Nanotechnology, Department of Chemistry, University of Oslo, P.O. Box 1033, Blindern, 0371, Oslo, Norway
[b] Faculty Section Storage of Electrochemical Energy, Radiation Science and Technology, Faculty of Applied Sciences, Delft University of Technology, Mekelweg 15, 2629, JB, Delft, the Netherlands
[c] Centro de Investigación Cooperativa de Energías Alternativas (CIC energiGUNE), Basque Research and Technology Alliance (BRTA), Alava Technology Park, Albert Einstein 48, 01510, Vitoria-Gasteiz, Spain
[d] ALISTORE European Research Institute, FR CNRS 3104, 80039 Amiens Cedex, France
[e] Department of Battery Technology, Institute for Energy Technology, P.O. Box 40, NO-2027 Kjeller, Norway

ARTICLE INFO

Keywords:
Li-ion batteries
Na-ion batteries
Cathodes
Antiperovskite
Cation disorder

ABSTRACT

Metal-ion batteries, particularly lithium-ion (Li-ion) and sodium-ion (Na-ion) batteries, are currently among the most compelling technologies for energy storage. However, the growing demands driven by wide implementation of batteries in multiple applications call for further improvements of energy and power densities. Despite the incredible developments in this field observed over the past decades, the innovation of new active materials for metal-ion batteries has seen only modest progress, with primary focus on the optimization of already existing materials. The recent discovery of cathode materials with antiperovskite structure signals a promising direction for the creation of relatively simple materials geared towards electrochemical energy storage. These materials can be synthesized through relatively simple chemical processes using abundant elements and could offer stable electrochemical performance. Even though the number of reported examples is still limited, the structural flexibility of these materials offers multiple possibilities for tuning the chemical stability, operating voltage and capacity. This perspective provides a summary of the latest advancements in the field of antiperovskite active materials, highlighting both the advantages and the challenges associated with their integration into metal-ion batteries, and suggests possible future research directions towards practical implementation of this promising yet underexplored class of materials.

1. Introduction

The evolution of materials science progresses in steps – a discovery of new materials with new properties attracts a lot attention focused on exploration of properties and various structural modifications, leaving the materials' discovery somewhat behind. Accordingly, the rapid development of battery chemistries in 20th century was primarily due to the discovery of several classes of intercalating compounds as cathode materials, which ultimately led to the speedy commercialization of Li-ion batteries (LIBs) [1–3].

While the current state-of-the-art anode materials for LIBs are primarily represented by graphite and graphite-silicon composites, a plethora of anode materials are suggested to improve modern LIBs [4]. However, the cathode chemistries for LIBs are primarily represented by 3 classes of materials: [5,6]

a) Layered oxides – Li_xTMO_2 (*TM* is a transition metal) with distorted rock-salt structure and the parent material $LiCoO_2$ [7], which resulted in the further development of state-of-the-art commercial NMC ($LiNi_xMn_yCo_{1-x-y}O_2$) and NCA ($LiNi_xCo_yAl_{1-x-y}O_2$) materials. Research efforts have recently focused on Ni-rich and Mn-rich compositions to reduce the share of Co, as well as Li-rich layered oxides which offer larger capacities involving anionic redox in addition to the TM redox activity.
b) Spinel oxides – $LiTM_2O_4$ offer high-operating-voltage Co-free alternatives. $LiMn_2O_4$ is commonly used in blends with NMC/NCA to gain

* Corresponding authors.
E-mail addresses: tian.dai@kjemi.uio.no (T. Dai), T.Famprikis@tudelft.nl (T. Famprikis), Alexey.Koposov@kjemi.uio.no (A.Y. Koposov).

https://doi.org/10.1016/j.ensm.2024.103363
Received 15 February 2024; Received in revised form 19 March 2024; Accepted 20 March 2024
Available online 21 March 2024

power performance. Cationic substitutions led to the development of spinel LMNO ($LiMn_{1.5}Ni_{0.5}O_2$), which is currently on the pathway to commercialization [8].

c) Polyanionic compounds – $Li_xTM_y(X_nO_m)_z$ ($X = P$, S, Si, …) encompass a large variety of structures and compositions that enable to tune the material's properties. The popular commercial choice of olivine (triphylite) $LiFePO_4$ delivers lower energy density than layered and spinel oxides but competes in sustainability and safety [9,10].

In addition to these 3 main classes of compounds, recently emerged conversion cathodes also showed great promise, however possible regulations regarding fluorine chemistry in Europe raise a concern of potential applicability of these materials in practical batteries [11].

The concepts developed for LIB were further extended to other battery chemistries, such as Na-ion batteries (NIBs), for which three main classes of commercially available cathode materials have been also adopted [12–16]:

a) Layered oxides with a chemical composition Na_xTMO_2 where Na-ions can migrate between rigid layers of TMO_2 [17].
b) Polyanionic compounds, with in particular $Na_3V_2(PO_4)_2F_3$ which forms a 3D structure with Na containing interconnecting channels, where the Na-ion can migrate [18].
c) Prussian blue analogues (PBA) - $Na_xTM[TM'(CN)_6]_{1-y}\bullet zH_2O$. PBA offer an open 3D structure of high crystallographic symmetry with where Na can migrate isotropically (3D) [12–14].

The abovementioned classes of cathode materials for both LIBs and NIBs have different advantages and disadvantages, but a detailed comparison is beyond this text to describe. Noteworthy, most of these materials have been adopted in commercial batteries or prototypes [15,16]. As a result of this successful implementation, further optimization of the cathode materials for LIBs and NIBs was carried out using a few selected strategies – doping, stoichiometry manipulations, coating, and microstructure engineering [19]. These strategies are generally applied to improve the overall cycling stability and electrical conductivity of cathode materials, eliminate the cation dissolution during cycling, and suppress the electrolyte decomposition during formation of cathode electrolyte interphase (CEI). Beyond the ongoing optimization of the current cathode Li-and Na-ion chemistries, the search for new materials remains, however, critical to respond to the current challenges of the battery field. In particular, new high-energy cathode materials obtained through inexpensive methods using abundant elements are needed to reduce the industrial dependency on critical materials and reduce carbon footprint of modern batteries.

Recently discovered compounds with antiperovskite (AP) structure and general formula of A_2TMChO (*A*: alkali metal, *TM*: transition metal, *Ch*: chalcogenide) represent a new and potentially promising class of cathode materials for LIBs and NIBs. Initially demonstrated in LIBs, AP cathode materials are relatively easy to synthesize, and offer high theoretical capacities (ca. 227.5 mAh/g or 455 mAh/g for Li_2FeSO, depending on if one or two Li^+ are extracted per formula unit, respectively). Although it is yet to be demonstrated, the possibility of extracting two Li^+ per formula unit is very attractive, since it would make AP materials far more competitive than other currently available cathode materials. Extraction of a single Li^+ positions AP materials in the same league as $LiFePO_4$ (LFP, 170 mAh/g), being slightly overperformed by $LiCoO_2$ (LCO, 274 mAh/g) and nickel-rich nickel manganese cobalt (NMC622, 276 mAh/g) considering capacity only [5,6,20]. Extraction of even a single Li^+ from AP formula unit makes these materials competitive in terms of energy density (c.a. 495 Wh/Kg for Li_2FeSO, 540 Wh/Kg for LFP, and 800 Wh/Kg for NMC811)[21]. The disordered cubic structure of the reported AP materials demonstrates a great chemical flexibility and can be prepared using abundant elements, avoiding the Critical Raw Materials such as cobalt and nickel. Upon cycling, this cubic structure results in isotropic and limited volume changes upon (de)lithiation, which prevents structural degradation and benefits extended cycle life [19,22-25]. To reflect the growing interest to this class of materials, the present perspective provides an overview of the current achievements in the field of AP cathode materials and highlights the research challenges, which should be addressed to make these promising compounds attractive for practical application [5,6,19,20,22-25].

2. Recent development of cathode materials with AP structure

To date, a variety of AP materials have been successfully synthesized and evaluated, primarily aiming to explore their potential as solid-state electrolytes for Li- and Na-based batteries [26–31]. Yet, thanks to the incorporation of redox active transition metals, Li_2TMChO was shown to reversibly intercalate Li^+ [32,33], unveiling a new family of promising cathode materials for LIB and NIBs.

2.1. Structure of A_2TMChO and their derivatives

Li-based APs as potential cathode materials were first reported in 2017. The initial synthesis of Li_2TMChO was inspired by the discovery of cation vacancy ordered AP ($\square Fe_2$)SeO ($\square$ = vacancy) [34]. Fe^{2+} occupies the center of four out of the six faces of an Se_8 cube of an idealized AP unit cell (Space group: Pm-3 m) to form an $OFe_4\square_2$ octahedron packing (Fig. 1b), where the vacant sites provide a possibility for Li^+ insertion. Li^+ and Fe^{2+} are similar in size (Li^+: 0.76 Å, VI-coordinated; Fe^{2+}: 0.78 Å, VI-coordinated at high-spin state[35]) thus, one Fe^{2+} can be replaced by two Li^+ simultaneously filling the structural vacancies. As a result, the two cations (Li^+ and Fe^{2+}) are randomly distributed within the OFe_2Li_4 octahedral vertices. This allows isotropic 3D Li^+ diffusion and minimal volume change upon extraction of Li^+, making them cation-disordered cathode materials similar to those in spinel $Li_{1+x}Mn_2O_4$ and disordered rock-salt materials [23,36,37]. The X-ray diffraction (XRD) pattern of AP Li_2FeSO is shown in Fig. 1a, and the corresponding general 3D crystal structure is shown in Fig. 1b-d, where the O^{2-} anions and the Ch^{2-} (chalcogenide) anions are 6-fold coordinated and 12-fold coordinated with either Li^+ or TM^{2+}cations, respectively. Such APs inherit the flexible structural features of the conventional perovskites, which accommodate vast chemical modifications, structural diversity, and tailored properties. The 4H structure of Li_2FeTeO is based on 4 hexagonally close-packed layers (ABAB) of (Li_2Fe)-Te, where O^{2-} occupies 1/8 of the octahedral voids, with only Li/Fe) as closest neighbors. These OLi_4Fe_2 octahedra share faces along the unique (c) axis. The cations occupy two different Wyckoff positions: one being fully occupied by lithium, and the other $Li_{0.33}Fe_{0.67}$. To date, only Li-based APs have been reported, even though the AP structure should be capable to accommodate other alkali-metal cations, such as Na, as long as appropriate *TM* and *Ch* combination is selected. Na-based APs, such as Na_2TMChO, would indeed be attractive cathode materials for NIBs. Although there is no report of successful synthesis of Na_2TMChO, replacing Li^+ in the Li-based APs with Na^+ was proposed by electrochemical delithiation followed by electrochemical sodiation [35]. This approach could provide an access to more Na-containing APs and serves as a proof of principle that Na-based APs are plausible. However, anticipated formation of $Na_xLi_{1-x}FeSO$ structure was only proposed based on electrochemical measurements, while no structural characterization was provided in the original work.

Ion conduction through the AP structures is understood to proceed similarly to the analogous A_3OX and A_2OHX antiperovskite solid-state electrolytes that have been recently studied [27–29]. Ion hoping is rationalized through migration between adjacent sites along the body diagonal of the cubic lattice (i.e. along the oxygen octahedral edges in Fig. 1b) in the presence of vacancies. For the cathode materials the vacancy concentration is a function of state of charge and, thus, the ionic conductivity is expected to evolve during operation, which is consistent

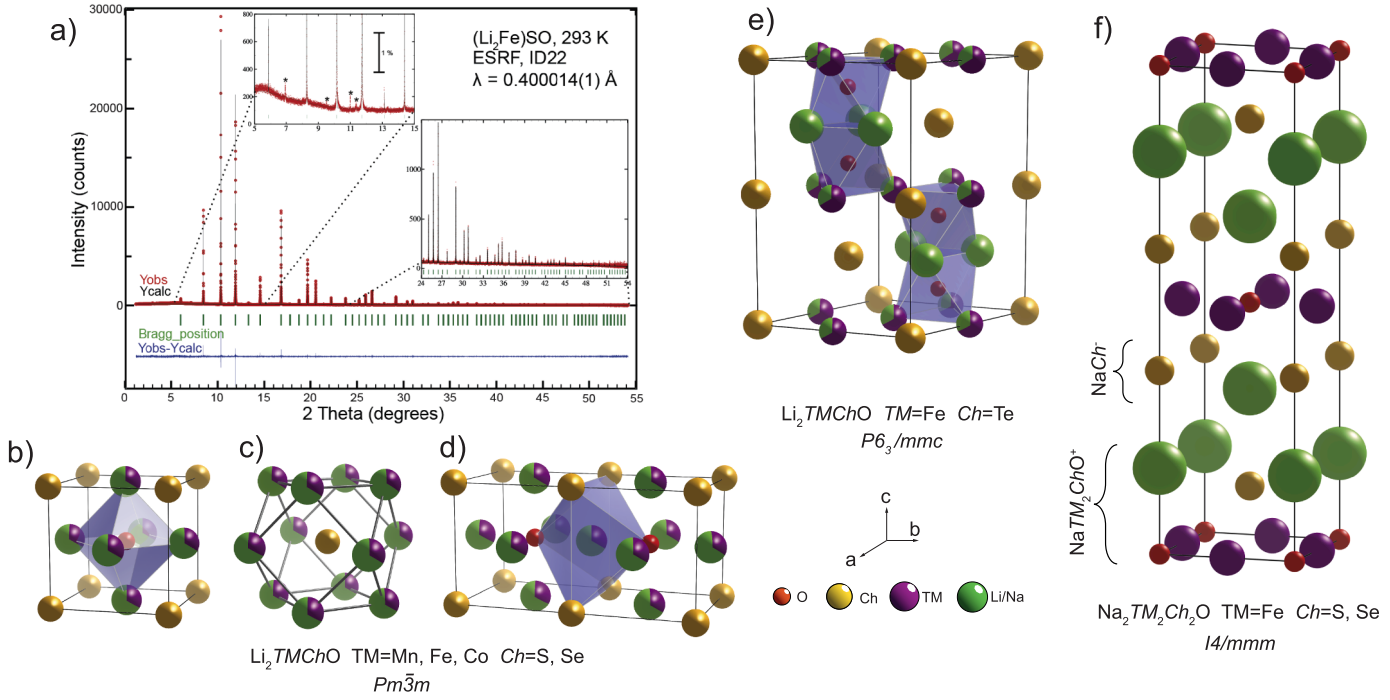

Fig. 1. a) XRD pattern of Cubic AP Li_2TMChO, adapted with permission from {Inorg. Chem. 2018, 57, 13,296−13,299}. Copyright {2018} American Chemical Society; b-d) Crystal structure and O-Li_4TM_2 octahedral packing configurations, *Ch* coordinates, and *TM* coordinates of cubic AP Li_2TMChO; e) Crystal structure of 4H-hexagonal Li_2TMChO; f) crystal structure of ARP $Na_2TM_2Ch_2O$; Crystal structures were visualized using Vesta [45].

with initial diffusivity results from galvanostatic intermitted titration technique (GITT) measurements [35]. Furthermore, the chemical modification strategies reported for the solid-state electrolytes such as doping on the cation and anion sites can be directly transferable to the antiperovskite electrode materials [38–40].

A similar, yet more complex variation of AP class of cathode materials is the Anti-Ruddlesden-Popper (ARP) structure [41,42]. In contrast to APs – only Na-based ARP compounds were successfully synthesized and electrochemically evaluated (e.g. $Na_2Fe_2S_2O$ and $Na_2Fe_2Se_2O$), but no Li-based ARP compounds were reported [43,44]. The ARP structure is described in the space group *I4/mmm* and consists of alternating $(NaTM_2ChO)^+$ and $(NaCh)^-$ layers stacked along the *c* direction, as shown in Fig. 1f. Despite the presence of AP fragments in the ARP phase, cation-disorder has not been reported for ARPs. Unlike for disordered APs, in ARPs Na^+ take the opposite vertices while the Fe^{2+} take the square planer coordination in a Na/Fe-O octahedral packing configuration. ARP structure infers a 2D Na-ion diffusion path (along the Na-rich planes), different from the 3D Li-ion diffusion path in AP structures.

2.2. Cation disorder in A_2TMChO materials

Most of the conventional LIB cathode materials often exhibit phase transitions upon (de)lithiation, which may negatively affect the cycling stability. In contrast, cathode materials presenting cation disorder (such as APs) may offer an alternative approach to gain structural stability upon cycling. Li^+ and TM^{2+} share the same site in the Li_2TMChO structure, and this disorder at the cationic site is a key aspect of the AP structure and critically linked to the electrochemical behavior. The multitude of possible local Li^+ environments in AP structure translates to a distribution of energies (chemical potentials) for Li^+. As a consequence, a distribution of localized potentials (voltages) leads to the characteristic 'slopy' cycling profile of disordered cathodes (as opposed to flatter plateaus of more ordered materials, e.g., LFP). Such structural disorder would influence the possibility of extracting Li^+ from AP leading to different capacities and rate capabilities. Therefore, a detailed understanding and description of (possibly correlated) disorder in AP cathodes is of particular importance [46,47].

Coles et al. computationally examined local ordering in the archetypical composition Li_2FeSO, showing the local correlation of Li/Fe cation disorder, i.e. it deviates from complete randomness and, thus can, be statistically described based on preferred motifs [48]. Specifically, the octahedral oxygen coordination is dictated by cation sites, thus, the nominal stoichiometry of Li_2FeSO is preferred with ca. 70% of oxygen ions coordinated within OLi_4Fe_2, and the remaining oxygen ions equally distributed within OLi_5Fe_1 and OLi_3Fe_3 local environments. That arrangement is in strong contrast to an initially assumed random cation distribution, where all possible OLi_xFe_{6-x} environments would be represented. Furthermore, the *cis*-OLi_4Fe_2 is preferred over the *trans*-OLi_4Fe_2, leading to the configurational underconstraint at the origin of long-range disorder as illustrated in Fig. 2. Each subsequent *cis*-OLi_4Fe_2 unit can be linked to the next one in multiple ways (configurational underconstraint) leading to long-range Li/TM disorder, while maintaining the local-range *cis*- correlation. The first *ex situ* pair-distribution function (PDF) analyses of cycled samples performed by Deng et al. [49]. indicates that the local ordering changes upon cycling. Furthermore, the study shows strong indications that local ordering and its irreversibility could be a function of composition, with Mn-containing Li_2FeSO showing quite different local structure and evolution compared to the pristine Li_2FeSO compound. These results lay the groundwork for modeling the cation distribution in AP cathode materials, and how that can be controlled by synthesis [48,49]. Such control of the local ordering provides a pathway to tailor the electrochemical behavior, even for materials with identical chemical composition.

2.3. Chemical stability

Chemical stability of the active material, in pristine and intermediate states, is of great importance for a stable battery performance, and essential for keeping a battery in a safe and stable working condition. Furthermore, chemical stability of a pristine material may affect its processability, making it potentially problematic if a special

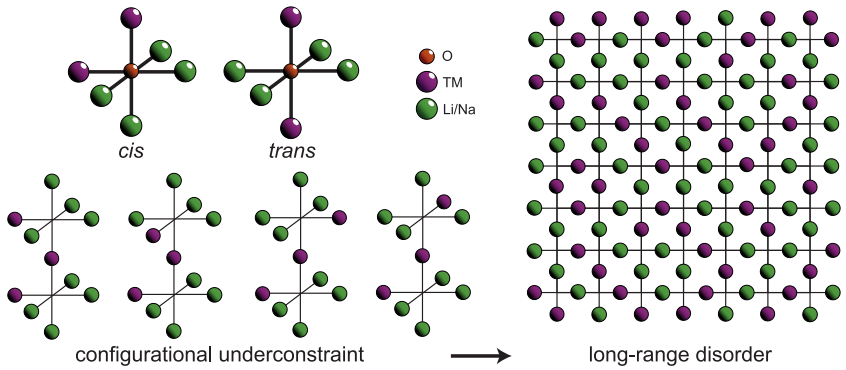

Fig. 2. *Trans*- and *cis*- coordination of O-Li_4Fe_2 structural unit, and schematic representation of long-rage disorder. Adapted from Coles et al. [48].

environment is required for its handling and battery manufacturing. While the conventional Goldschmidt tolerance factor cannot be directly adopted for predicting cation disordered AP structures, the stability and ionic transport of the parent compound - Li_2FeSO were evaluated through a set of DFT calculations by Lu et al. [50]. Specifically, it was demonstrated that the experimentally observed AP phase likely originates from entropy stabilization and sluggish decomposition kinetics, i.e. decomposition of Li_2FeSO into FeS, Li_2S and Li_2FeO_2. However, another work, based on an alternative computational approach, suggested Li_2FeSO to be intrinsically stable, indicating the decomposition process still needs to be experimentally verified [51]. To date, there is no experimental evidence proving or disproving instability of AP structures under controlled atmosphere making it reasonable to assume that chemical stability is not an issue for these materials. Several publications reporting successful preparation and manipulation of Li_2TMChO compounds indirectly confirms their practical stability under controlled atmosphere.

The reported Li_2TMChO compounds tend to absorb H_2O and O_2 when exposed to moist air, possibly due to surface polarity induced by unbalanced local charge environment [52]. This indicates instability towards air and moisture for at least some of AP materials and, thus, the environment for handling AP materials must be controlled from synthesis to battery assembling. Specifically, Lai et al. [32]. reported the decomposition of Li_2FeChO ($Ch = S$, Se) in moist air, when both water and oxygen were proposed to participate in the reaction. A rapid decomposition of Li_2FeSO into several phases was observed after only 90 min of exposure to moist air, forming Li(OH), Li(OH)·H_2O, and FeS as main products. This was attributed to possible Li^+ leaching and formation of Li(OH) and Li(OH)·H_2O at the particles surfaces [20]. Such decomposition in moist air could be easily evidenced by observing the color change from initial brown to black within a few minutes. In addition, toxic H_2S can also be released upon decomposition. A similar process was observed for Li_2FeSeO, however, it progresses substantially slower than that for the sulfide oxide due to the more ionic character of sulfide oxides as compared to selenide oxides. The sensitivity to dry air was also evaluated: Li_2FeSeO was shown to be stable in dry air at room temperature over the course of 5 h as evidenced by XRD, where no significant new diffraction peaks or peak shifting were observed [32].

Mohamed et al. further confirmed improvement of Li_2FeChO ($Ch = S$, Se) stability by increasing the Se content in the parent sulfide [20]. Such improvement could be possibly explained by the lattice distortion caused through partial substitution of S with Se, which increases the tolerance factor *t*, and,thus, resulting in an increase of energy barrier for Li^+ migration and leaching of $Li^+$from the AP structure upon exposure to water and oxygen. The instability in moist atmosphere was also observed for other *TM*-substituted Li_2TMChO (TM = Mn, Co, $Ch = S$, Se), with Se-based compounds being more stable than S-based materials. A partial substitution of Fe with other transition metals such as Mn and Co results in decreased air and moisture sensitivity, similar to what is observed for delafossite $Li(Ni_{0.8}Co_{0.15}Al_{0.05})O_2$, suggesting that the compounds with mixed composition exhibit better structure stability [53,54]. Overall, the potential sensitivity of AP materials to the ambient condition may represent a severe concern to address if these materials will reach commercialization level.

2.4. Synthesis and characterization of AP Li_2TMChO materials

At present, two main approaches for the synthesis of AP Li_2TMChO materials are generally adopted: 1) single-step solid-state synthesis and 2) mechanochemical synthesis. The solid-state reaction remains a popular choice for synthesizing AP materials, offering a simple approach with an ability to create tailored materials with high degree of crystallinity for diverse energy storage applications, while mechanochemical synthesis enables low energy consumption, potential mass production, and control of particle size distribution. The synthetic methods and respective chemical compositions are schematically shown in Fig. 3.

Lai et al. reported the first single-step solid state synthesis of Li_2FeChO ($Ch = S$, Se, Te), opening the field of AP materials for cathode applications [32]. The synthesis was based on the following reaction utilizing lithium oxide and elements: $Li_2O + Fe + Ch = Li_2FeChO$. However, it was demonstrated that commercial Li_2O contains small amounts of Li(OH) and Li_2CO_3, and a thermal decomposition of Li_2O precursor should be conducted prior to the main synthesis stage to improve the phase purity of the final product. Additionally, excess of Li_2O (usually 5% molar) compensates for the losses during the reaction and increases the crystallinity of Li_2FeChO. For a typical synthesis, the precursors are mixed, filled into a corundum crucible, which is then loaded inside a silica ampule. The ampule should be sealed using a burner to ensure a static vacuum inside and then heated up to 650 - 750 °C. The reaction proceeds over the course of 2–10 h (different times were reported by different authors) followed by a quenching process, which was suggested to prevent the formation of additional phases. Both Li_2FeSO and Li_2FeSeO synthesized through this method exhibit cubic AP structure, with a $Pm\bar{3}m$ space group, as could be expected, the cell volumes increase with a change of chalcogenide, with sulfide having the smaller and selenide the larger unit cells, respectively.

Several modifications have been proposed for further tunability and improvement of the solid-state synthesis. For instance, it was found that increasing the initial argon pressure in the reaction ampule to 0.5 bar would prevent the sublimation and migration of sulfur inside the crucible, which often leads to formation of impurities [54]. Similarly, Coles et al. reported the synthesis approach based on annealing, when the precursors were directly placed in a preheated furnace at 750 °C. The material was annealed at this temperature for 4 h, with intermittent grinding and subsequent quenching the sealed ampule in ice water [48]. In addition, Miura et al. utilized an argon tube furnace for calcination under ambient pressure for the synthesis of Li_2FeSO [55]; this procedure simplified the complex calcination steps at a low pressure. This versatile solid-state approach was further deployed for studies of APs with different chemical compositions, such as Li_2TMChO (TM = Mn, Co; Ch =

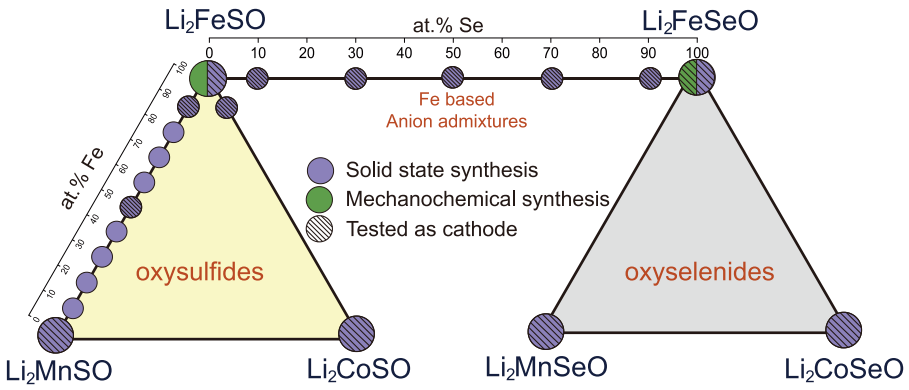

Fig. 3. Schematic illustration of the experimentally reported Li-ion AP cathode materials with different *TM*s and *Ch*s to date and corresponding synthesis route. The two triangles refer to S- and Se-based compounds, respectively, and the vertices indicate *TM* end-members. The sidelines correspond to the atomic percentage of each *TM* or *Ch*.

S, Se) as illustrated on Fig. 3. All these reported compounds are reported to crystallize in cubic AP structures, further demonstrating the chemical flexibility of AP structure and possibilities to prepare new compounds. Although the electrochemical performance varies for different chemical compositions, the partial substitution of *TM* cations was shown to be an effective approach for improving not only stability, but also electrochemical performance of Li_2*TMCh*O [50].

Despite the seamless simplicity of the solid-state approach, few major disadvantages of this synthetic procedure are worth highlighting: a) high temperature is required for the reaction results in sizeable energy consumption, b) the difficulties to control the particle morphology and size distribution, and c) questionable scalability given the sensitivity of Li_2*TMCh*O to ambient humidity. For Li_2FeSeO synthesized through solid-state route, the particle size ranges from a few micrometers to tens of micrometers [56]. The latter is of particular importance for electrochemical properties. It should be also noted that experimental conditions vary from one work to another, making the synthesis challenging for the newcomers to the field. In response to these issues, the mechanochemical synthesis was proposed as an alternative for the preparation of AP materials. This approach has provided the benefit of producing sub-micron particles with appreciable amount of structural disorder and improved ionic conductivity [57–59]. Mohamed et al. [60]. and Singer et al. [61]. reported the single-step mechanochemical synthesis of Li_2FeSO and Li_2FeSeO through ball-milling from the same starting materials as those used for the solid-state synthesis, with the optimization of ball-milling parameters the desired phase of Li_2FeSO is yielded, however several impurities, such as sulfur, FeS, $LiFeO_2$, etc. were found to be present in the final product. The purity of Li_2FeSO can be improved with the increase of milling time up to 85 h as was confirmed by *ex situ* XRD measurements, with Fe metal as the primary secondary phase. To further increase the phase purity and crystallinity, post-treatments at different temperatures (300–500 °C) were also studied.

For Li_2FeSO synthesized through mechanochemical method, the particle size is evenly distributed and reduced to a few micrometers compared to solid-state synthesis [60]. However, while the heat treatment improves the crystallinity, small particles formed by ball-milling have a tendency to form larger secondary particles during this process. The influence of the (primary and secondary) particle size distribution on electrochemical performance remains to be studied [61].

XRD analyses of Li_2*TMCh*O indicate the cubic structure for all reported AP cathode materials with the lattice parameter increasing through *TM* = Co-Fe-Mn. It is worth noticing that in case of $Li_2Fe_xMn_{1-x}SO$ additional reflections were found in the XRD pattern which were indexed as $2 \times 2 \times 2$ and $6 \times 6 \times 6$ superstructures [49]. The existence of superstructures and their influence on structural stability of the materials upon electrochemical cycling are still not well documented.

2.5. Electrochemical behavior of A_2*TMCh*O cathode materials

Li_2*TMCh*O cathodes distinguish themselves from state-of-the-art LIB cathodes by its relatively high specific capacity (theoretically, 227.5 mAh/g or 455 mAh/g for Li_2FeSO for one or two Li^+ extracted per formula unit, respectively) and relatively low working potential (average voltage ~2.1 V vs Li/Li^+). Fig. 4a showcases the specific capacity of Li_2FeSO achieved experimentally for the first cycle at slow rate (C/10 or slower) in earlier works demonstrating the ability to achieve relatively high specific capacities of about 220–270 mAh/g in the voltage window 1.0 to 3.0 V vs Li/Li^+, corresponding to the cycling of 1–1.2 lithium per formula unit [20,35,49,54,61,62]. Fig. 4b illustrates the working potentials and specific capacities of well-studied families of cathode for LIBs as well as the newly discovered Li_2*TMCh*O. Reported electrochemical data suggest that the potentials of the redox processes of Li_2*TMCh*O (especially those on charge) progressively change resulting in an average potential roughly around 2 V. At low technology readiness level, one can hope to improve the voltage hysteresis between charge and discharge by electrode optimization. For the sake of comparison, the average potential for Li_2FeSO (about 2.1 V) in Fig. 4b is obtained by averaging first charge and discharge capacities from Mikhailova et al. (Fig. 4c) [38].

From the perspective of chemical composition, oxychalcogenide materials are different from layered oxide cathode materials such as LCO ($LiCoO_2$), LMO ($LiMnO_2$) or NMC ($LiNi_xMn_yCo_{1-x-y}O_2$), by the replacement of a chalcogen element in place of an oxygen. The introduction of the less electronegative chalcogen together with the use of $Fe^{2+/3+}$ redox process hence lowers the potential of the oxysulfide and oxyselenide AP materials. As expected, Li_2FeSO also present a lower electrochemical potential than the iron-based $LiFePO_4$ (~3.45 V vs. Li/Li^+), which benefits from the high inductive effect of the polyanionic group PO_4 [9]. The comparatively low potential of AP Li_2Fe*Ch*O cathodes is compensated by its high specific capacity and makes it competitive in terms of energy density with other state-of-the-art materials, which energy densities are in the range of 600–800 Wh/kg, considering ~1.2 Li^+ extracted per formula unit. In addition, the low operating potential of the AP Li_2*TMCh*O cathodes may also allow their implementation with battery materials that are unstable at higher potentials. For instance, argyrodite Li_6PS_5Cl and similar sulfide-based solid-state electrolytes are unstable above 2.5 V vs Li/Li^+ [63]. In fact, Miura et al. have demonstrated the suitability of Li_2FeSO in a solid-state battery using argyrodite as a solid electrolyte [62,63].

The as-synthesized materials contain two Li^+ per formula unit and the following formal charges can be assigned: $Li_2^+TM^{2+}Ch^{2-}O^{2-}$. The overall delithiation reaction of the AP cathode can be expressed as [20]:

$$Li_2TMChO \rightarrow Li_{2-x}TMChO + xLi^+ + e^-,$$

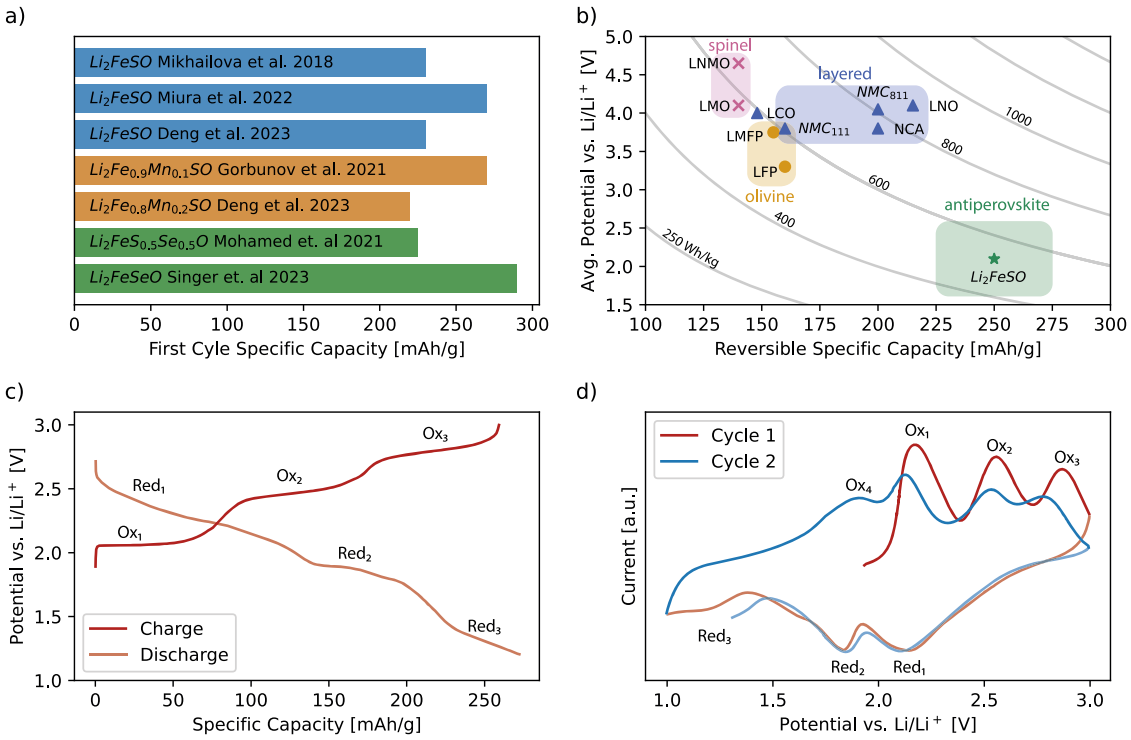

Fig. 4. (a) A comparison of specific capacities for the experimentally reported AP Li_2TMChO materials measured during first charge at slow cycling rate (C/10 or lower)[20,35,49,53,54,62] (b) schematic illustration of operating potential and specific capacities of families of cathode materials[64] and AP materials - Li_2TMChO; (c) charge/discharge curves for Li_2FeSO (adapted from Gorbunov 2020)[53] (d) cyclic voltammetry of a Li_2FeSO cell at a sweeping rate of 0.05 mV/s (adapted from Mikhailova 2018)[35].

with $0 < x < 2$ (theoretically).

Studies have shown both cationic and anionic redox from the transition metal and chalcogenide, respectively, contribute to the electrochemical reaction of up to 1.2 lithium [20]. While redox activity from *TM* is clearly defined – TM^{2+}/TM^{3+}, the redox process corresponding to chalcogenide activity could be formally assigned to Ch^{2-}/Ch^0. However, this process is yet to be confirmed, even though the formal oxidation states at various states of charge have been studied through a combination of X-ray photoelectron spectroscopy (XPS)[35], X-ray absorption spectroscopy (XAS)[20,35,53,54] and Mössbauer spectroscopy[35]. Oxygen has been shown, by XPS, to retain its oxidation state of -II even when cycled up to 3.0 V vs Li/Li^+ [35].

Overall, Li_2TMChO cathodes have similar electrochemical behaviours with varying *TM* and *Ch*. The primary difference between these materials is the redox potential, as expected from the composition differences. A preliminary identification of the electrochemical reactions can be made on cycling experiments of Li_2FeSO performed by Gorbunov et al. and Mikhailova et al. as illustrated by a voltage curve[53] (Fig. 4c) and a cyclic voltammetry curve[35] (Fig. 4d). The electrochemical process can be described by three plateaus in charge curve (Fig. 4c), or by three oxidation peaks on the cyclic voltammetry curve (Fig. 4d). The first two peaks to appear (labelled "Ox1" and "Ox2" at about 2.15 V and 2.55 V vs Li/Li^+, respectively) are associated to a Fe oxidation from +II to +III as evidenced by XPS[35], XAS[20,35,53,54] and Mössbauer spectroscopy[35]. The third oxidation peak (labelled "Ox3" at about 2.85 V vs Li/Li^+) was attributed to partial anion redox of sulfur as evidenced by XPS[35,49,61]. Similar observations can be made on the electrochemical features of compositions containing manganese [53,54], cobalt [54], or selenium [20,32,33,56,61].

During discharge, the three redox peaks (labelled "Red1", "Red2" and "Red3" in Fig. 4c and 4d) appear broader than the oxidation peaks. This difference in shape can be explained by a slower lithium diffusion during the discharge, as indicated by GITT measurements using various cathode compositions [20,35,49,53,54]. Although the redox couples can be identified by confining the potential window, as demonstrated by Singer *et al.* for Li_2FeSeO [61], the reduction processes alone have not been investigated. The discharge processes exhibit very different thermodynamic/kinetic characters than the charge processes.

From the second charge onwards, a fourth oxidation process appears (labelled "Ox4" at about 1.90 V vs Li/Li^+ in Fig. 4d), before the initial Open-circuit voltage (OCV), which has yet to be studied by spectroscopic techniques as the other oxidation processes have. The subsequent electrochemical cycles lead to increase of broadening and decrease of the peak intensities. This indicates a change in the energies of electrochemical reactions during cycling, which may be caused by a change in the local structural environment, amorphization of AP material or a formation of phases not participating in the electrochemistry, as was suggested by several previous works [32,35,49,53,54,60].

The initial capacity when cycling between 1.0 to 3.0 V vs Li/Li^+ is *quasi* reversible during short cycling but fades noticeably over the course of longer cycling tests [35,49,53,54,56,61]. For example, Mikhailova et al. measured a decrease in specific capacity from an initial 227 mAh/g to 150 mAh/g after 50 cycles at rate of C/10 for Li_2FeSO [35]. Such capacity fading could be rationalized through irreversible reactions. Singer et al. proposed that capacity loss is caused by an irreversible transformation of Li_2FeSeO into $Fe_{1-x}Se_x$ (with $x = 0.21–0.29$) at about 2.6 V vs Li/Li^+ [61]. They were able to achieve a much better capacity retention at the cost of average capacity (*c.a.* 95 mAh/g to 80 mAh/g after 100 cycles at 1 C) by heat treating the cathode material and lowering the upper limit of the potential window from 3.0 V to 2.5 V vs Li/Li^+. Further studies on each reaction mechanism are needed to better understand the causes for capacity fade and develop strategies to take achieve reversible and high practical specific capacity.

The electrochemical performances greatly depend on the materials, cell design and test procedure, as they affect the Li^+ diffusion and kinetics of the redox reactions. Several studies show the rate capability of Li_2FeSO at cycling rates up to 1 C [20,32,33,35,49,54,56,61,62], but

discrepancies in the cell making and testing make it difficult to compare electrochemical data between different publications. The Supplementary Information provides a comprehensive table of electrochemical cell materials and cathode processing. For example, Mikhailova et al. [35]. measured 200 mAh/g while Deng et al. [49]. measured about 20 mAh/g, both for Li_2FeSO at 1 C rate. For the same reason, the present review paper has not attempted to compare the electrochemical behaviours and performances of different compositions within the AP Li_2TMChO cathode family. It should be noted that factors linked to the cell making such as the effects of the electrolytes on the capacity fade, cathode-electrolyte interfacial reactions and solubility of the oxychalcogenide cathode material are not yet understood. All these factors emphasize the need to consider the effect of the electrochemical systems on the cycling data, to have a comprehensive understanding of the intrinsic electrochemical properties of the Li_2TMChO cathode family.

As stated in Section 2.1, the direct synthesis of a sodium member of the cubic AP family of cathode material (A_2TMChO, with A = Na) has yet to be reported. However, two recent publications have demonstrated successful synthesis of an electrochemically active ARP cathode materials (as a derivative of APs) for NIBs ($Na_2Fe_2S_2O$ by Gamon et al. and $Na_2Fe_2Se_2O$ by Gorbunov *et al.*) [43,44]. The ARP structure is different from the AP cathodes, so the electrochemical processes are expected to be different. However, comparing both families of iron-based oxychalcogenide materials may lead to pertinent understanding and discoveries for both classes of materials. $Na_2Fe_2S_2O$ and $Na_2Fe_2Se_2O$ have complex multistage charging curves and suffer from capacity fade. The initial capacities for $Na_2Fe_2S_2O$ and for $Na_2Fe_2Se_2O$ were reported to be 170mAh/g and 150mAh/g respectively, when cycling between 1.5 to 3.0 V vs Na/Na^+. Both publications suggested that the capacity fade is due to amorphization or irreversible deterioration of the structure. Both groups suggested that a better understanding of the local structure and amorphization during cycling is needed to achieve a significant practical capacity for the Na-based ARP cathode materials.

2.6. Mechanistic studies of A_2TMChO cathode materials

The complexity of the electrochemical processes observed for the AP oxychalcogenide materials results in poor understanding of their reaction mechanism. However, such knowledge is essential for assessment of the structural stability of intermediate phases formed during cycling, cation disorder, which are all in control of cycling stability and capacity of the AP materials as described in the Sections 2.2 and 2.5. To the

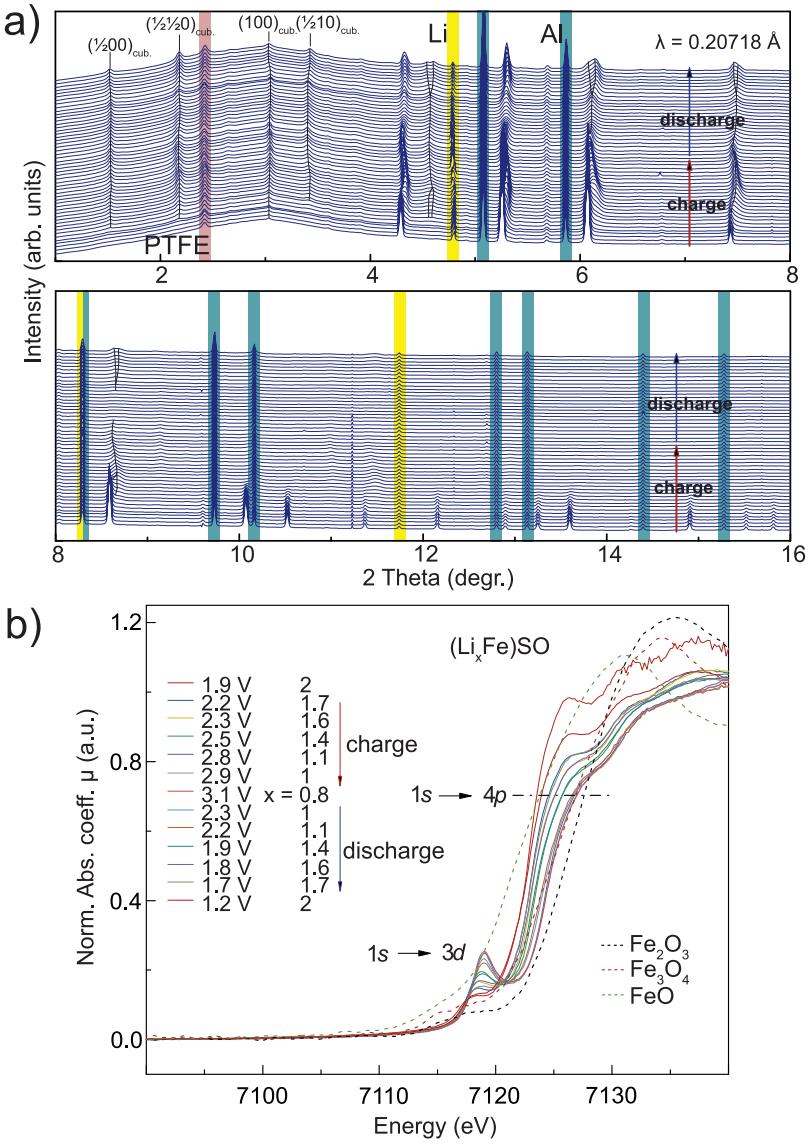

Fig. 5. (a) *Operando* XRD of Li_2FeSO cell during single charge and discharge; (b) *Operando* X-ray absorption spectroscopy near the Fe K edge. Adapted with permission from {ACS Appl. Energy Mater. 2018, 1, 6593−6599}. Copyright {2018} American Chemical Society.

present moment, only a few articles reported somewhat detailed insights into the operation mechanism of Li_2FeSO (Fig. 5a-b) [35,54], while the operational mechanisms of other AP and especially ARP representatives are still unknown.

The complex mechanism involving at least three distinct redox processes as discussed in Section 2.5 often results in the removal of more than 1 Li^+ per formula unit, which indirectly indicates the participation of chalcogenide. *Operando* XAS and *ex situ* Fe Mössbauer spectroscopy experiments confirmed a redox activity of iron (Fe^{2+}/Fe^{3+}) over the full voltage window 1.2–2.9 V vs Li/Li^+ during the first cycle which is expected by the analogy with other conventional Fe-based cathode materials. On the other hand, the removal of more than one Li^+ per formula unit can be only rationalized by a reversible oxidation of S^{2-}, as suggested by *ex situ* XPS and *operando* EXAFS [35]. However, the nature of the sulfides formed after the first discharge has not been unveiled. Furthermore, the participation of the chalcogenide in the redox process can also lead to additional distortion of the crystal structure creating difficulties for extensive characterization during cycling.

Operando XRD and *ex situ* Mössbauer experiments indicate that the $Li_{2-x}FeSO$ undergoes irreversible structural changes (distortion of the Fe environment) upon the first charge, that still need to be further understood and confirmed [35]. The high-spin state paramagnetic Fe^{2+} ion was indeed observed in both Li_2FeSO and Li_2FeSeO as evidenced by Mössbauer spectroscopy and XPS, respectively [35,56]. The crystallinity of the oxysulfide is altered during the first charge, and new reflections appear in the XRD patterns, that could be assigned to a superstructure with a doubling of the initial cubic unit cell, or to the formation of a new phase [35]. In addition, the evolution of the unit cell parameter of the AP phase follows opposite behaviors during the first and second oxidative processes. While *operando* XRD experiments on $Li_{2-x}[Fe_{0.9}Co_{0.1}]SO$ suggest similar reaction mechanism as that of $Li_{2-x}FeSO$, substituting Fe by Mn ($Li_{2-x}[Fe_{0.9}Mn_{0.1}]SO$ and $Li_{2-x}[Fe_{0.5}Mn_{0.5}]SO$) leads to a significant modification of the reaction mechanism, involving two phases with varying solubility limits over the first 0.8 Li exchanged [53,54].

2.7. Intermediate conclusions

AP oxychalcogenides A_2TMChO have emerged as promising candidates for energy storage applications, particularly as cathode materials in LiBs. The general crystal structure of APs allows for rich cation diversity on both *TM* and *Ch* sites and structural modifications, offering a wide range of compositions and properties. While more than a dozen of A_2TMChO materials was prepared and evaluated electrochemically, the focus has primarily been on Li-based APs, with significant attention given to elements like Fe and Mn due to their earth abundance and stable reversible capacities. Despite advances in Li-based APs, Na-based counterparts remain unexplored, representing a potential avenue for diversifying cathode materials for NIBs. If a good performance and a chemical flexibility of APs can be utilized in combination with Na, these materials will be extremely useful. The sensitivity to moisture for some of the AP oxychalcogenides may represent a legitimate concern, however, with ongoing investigations into substitutions, thermodynamic behaviors, and operando studies, AP materials hold a promise as versatile materials for next-generation energy storage technologies, with the potential to address current limitations and contribute to the evolution of battery technology.

3. Future directions/need for research

The field of AP A_2TMChO active materials is still at its infancy and thus it offers a variety of experimental possibilities not only in terms of analysis and electrochemical evaluation, but also in terms of materials discovery and development. The early work summarized above can serve as an inspiration for future research in this direction. In addition, the analysis of the literature above highlighted that the stability of some of the representatives within the AP class may raise a concern for their potential applicability within real batteries. The following section summarizes future research directions for these interesting yet understudied materials.

3.1. New compositions and structure derivatives

The inorganic chemistry of crystalline materials is strongly influenced by crystal structure parameters, which are often related to fundamental properties such as ionic sizes, oxidation states, preferable coordination, bonding type, electronic potential, and others. When focusing on the cubic AP structures, there are already well-established, geometrical preferences for a stable crystal lattice. The most cited one is the Goldschmidt tolerance factor [65], where the radii of involved ions are placed in a trigonometric calculation, maximizing the packing. It is often assumed that the bonding type is strictly ionic, making it possible to use the Shannon-Prewitt radii for tolerance factor calculations [66]. In the cubic AP structure, the *TM*-site is coordinated by 2 O and 4 *Ch* in a *trans*-like manner (Fig. 1d), thus, using the listed ionic radii, it is possible to estimate the space in the resulting octahedral coordination. If a is the cubic unit cell parameter, r_{Ch} is the radius of the larger chalcogenide ion, while r_O is that of oxygen (or smaller chalcogenide), the space in the center of the distorted octahedron is roughly a spheroid with specific axial length and width. For example, Li_2FeSeO has $a = 4.00$ Å, with $r_O = 1.40$ Å and $r_{Se} = 1.98$ Å, the possible *TM* space between O—O has a length of 1.2 Å and between Se-Se is 1.70 Å. Even though the space shows spheroid anisotropy, it allows for chemical flexibility and displacement from the high-symmetry position (in the center), especially in the *TM*-Se plane. Naturally, this should be considered when discussing the ionic conductivity of the cubic APs. However, from experiments, it seems as if the axial length is not a hard limit for the absolute size of the *TM* ion, as the reported [33] ions (ionic diameter in Å for high-spin) are Fe^{2+} (1.56 Å), Co^{2+} (1.49 Å), and Mn^{2+} (1.66 Å) [67], well above the strict ionic limit. Hence, it is evident that the bonding type contains significant covalent character. This is also valid when Li^+ (1.52 Å) occupies the site, and a displacement from the center position is most probably necessary to accommodate the size of Li^+, which is expected to have a more ionic bonding character, as compared to the *TM* ions. By this crude size-comparing method, there are many more options of ions that could occupy the *TM* site than originally proposed – *e.g.* Ni^{2+} (1.38 Å), V^{2+} (1.58 Å), Cr^{2+} (1.60 Å for high-spin) or Cu^{2+} (1.46 Å). However, the incorporation of the latter two is unlikely because of their redox instability towards Ch^{2-} (*Ch* = *S*, Se) - resulting in e.g. Cu^+ and Ch^-. Hence, Ni^{2+} should be a perfectly suitable candidate for the new AP materials. In contrast, the incorporation of Mg^{2+}, Zn^{2+}, and Cd^{2+} would also be possible from the structural perspective, but their thermodynamically stable binaries, MgO, Zn*Ch*, and Cd*Ch* increase the risk of secondary phases to form during synthesis. However, these possibilities are interesting only from the structural point of view, as they will not be practical for the application as active materials in metal-ion batteries. In the case of Na^+ (ionic radii = 1.02 Å), it is clear that this ion could be problematic for the cubic structure due to its size. Hence, it remains a challenge to determine if the AP structure can incorporate Na^+ or if other structures are formed, such as those of ARP [35,43,44].

While the chemical flexibility of A_2TMChO structure enables a wide selection of *TM* and *Ch* elements, studies were primarily limited to *TM* = Fe, Mn, Co and *Ch* = *S*, Se, Te. To further explore the AP chemistry the following design rules for a new cathode material should be considered: a) an element that can participate in a redox reaction within reasonable voltage window, b) covalent bonding type within the host lattice to assure stability, and c) a hollow atomic lattice with large enough migration paths for Li^+ or Na^+. All these chemical and structural prerequisites narrow down the possible chemistry.

The *TM*s in the AP structure could be used for controlling and modulating electrochemical properties and, thus, could possibly be chosen from a broad selection of electrochemically active transition metals (Cr, Mn, Fe, Co, Ni, Cu, *etc.*) and/or electrochemically inactive

elements (Zn, Mg, Ca, *etc.*). For Li-based APs, Fe and Mn have received more attention because they are earth-abundant elements and provide reasonable reversible capacities. Additionally, the overall charge must be adjusted to retain the AP stoichiometry, where both oxygen and chalcogenide have a nominal −II oxidation states, and Li/*TM* are expected to be in the +I/+II states, respectively.

Substitution at *TM* sites is particularly interesting for increasing structure stability and cycling performance of cathode materials. Enhancing the configurational entropy by elemental substitution can increase the cation disordering and induce more Li-rich configurations for fast Li^+ diffusion channels in the cation disordered rock-salt cathodes. DFT calculation conducted by Deng et al. [49]. suggested the substitution of Fe^{2+} with Mn^{2+} will increase cation disorder, creating more Li^+ enriched domains within AP crystal structure, which can potentially facilitate Li^+ diffusion. In addition, the Jahn-Teller distortion, which was reported in disordered rock-salt cathode materials due to the partially filled d-orbital in Mn^{3+} or Fe^{4+}, could also affect the structure and further hamper the electrochemical performance, which should be taken into account when considering *TM* candidates. Lu et al. [50]. predicted the substitution of a series of *TM* (Co, Cr, Cu, Fe, Mn, Mo, Ni, V) in Li_2*TM*SO, where it was suggested that the Fe and Mn versions show the lowest energy above hull (< 50 meV/atom), and Cr, Cu versions give the smallest bandgap (< 0.3 eV). According to their assessment, only the Fe and Mn could be prepared (as metastable < 100 meV/atom). However, their results have been challenged on both experimental and computational grounds; for instance, the Co-based AP was synthesized[33] even though Lu et al. labeled this compound as unstable. Computationally, their methodology has been criticized as incorrectly applying the "U" corrections needed for energy calculations involving transition metals, meaning that the resulting computed formation energies were not reliable [51]. A natural next step from the modeling point of view would be to simulate voltage profiles resulting from different physical orderings to help elucidate the electrochemical mechanism in conjunction with associated experimental investigations including advanced crystallographic- and *operando* studies [68]. Moreover, the admixtures of more than one cation at the *TM* site can result in more chemical stability and changes in operation voltage, which is a large chemistry research field to be explored. Mixtures of ions on the *Ch* site have already been reported but these parameters are still open for further exploration [20].

When focusing on the anion substructure within APs, *e.g.* Se^{2-} and O^{2-}, the structural resemblance with the CsCl-type structure is striking, which should be an important geometrical factor for the apparent stability of the AP structure. Disregarding the ionic charges for a moment, the corresponding ionic radii for the anions are Se^{2-} (1.98 Å) and O^{2-} (1.4 Å), giving an ionic size ratio of about 1.41. Comparing the ionic radii of Cs^+ (1.67 Å) and Cl^- (1.81 Å), presuming the same coordination number of 6 (8 is not listed for Cl^-)[66], it is possible to calculate a corresponding ratio to 0.92. Hence, it might be argued that the "small" O^{2-} ions could be the reason for the relatively large space available for the cations in the AP structure. Reinstating the charge into the discussion, the O^{2-} then keeps the Se^{2-} ion far apart for a relatively flexible cation lattice.

Structurally related to "conventional" perovskites are the Ruddlesden-Popper phases, which belong to a series of compounds, starting from X_2YO_4 (X = larger cation, Y = smaller cation) with many compounds in between before ending at XYO_3 (perovskite). This extension to crystal chemistry also allowed for the AP materials, e.g. in Ca_3ZO (Z = Ge[69], Sn, Pb[70]) to Ca_4Z_2O (Z = *P*, As, Sb, Bi)[71]. The possibility of this extension has been already theoretically considered, going through a series of compounds $(Li_2Fe)ChO$ – $(Li_2Fe_2)Ch_2O$ [41, 51], but needs to be experimentally verified. In addition, introduction of phosphorus (P)[71] in the AP cathode materials could be plausible because it does form the ARP phase Ca_4P_2O, and it has relatively low molar mass.

Zhu et al. undertook a search for other oxysulfide compositions in the Li-Fe-S-O phase space, using ab initio random structure searching [51]. They identified a multitude of compositions, most relevantly an ARP phase $Li_2Fe_2S_2O$ (i.e. Li_2FeSO + FeS) that was predicted to be stable (it should be noted that the Na analogues, i.e. $Na_2Fe_2S_2O$ and $Na_2Fe_2Se_2O$, have been already reported recently) [43,44]. The predicted Li-based compounds $Li_2Fe_2S_2O$ and $Li_4Fe_3S_3O_2$ were found to exhibit high theoretical capacity (260.6 mAh/g and 248.6 mAh/g, respectively), which makes them promising candidates for the future synthetic work.

The AP and ARP materials offer a variety of synthetic opportunities for the future explorations and structural modifications through substitution at the TM and Ch sites.

3.2. Need for operando characterization

The initial evaluations of the operation mechanism of AP cathode materials are not fully conclusive: the formation of additional phases and amorphous materials are yet to be comprehended. In addition, it should be noted that the operation mechanism of the Na-based APs and ARP compounds has not been investigated. Furthermore, the disordered structure of the AP compounds also leads to compounds with microstructural diversity formed during electrochemical cycling, that can be difficult to fully characterize, leading to different electrochemical behaviors/reaction mechanisms. However, one of the most important questions yet to be answered is how the participation of the chalcogenide ion in the electrochemistry affects the stability of the materials. The answer to this question requires the use of multiple experimental techniques, which can provide information about amorphous components and migration of Li-ions in the structure. The structures formed upon lithiation/delithiation, the cation disorder and products of the electrochemical reactions need to be investigated as they may affect the performance as a battery material. That calls for the use of such techniques as nuclear magnetic resonance (NMR) and pair distribution function (PDF). In addition, neutron scattering could prove valuable for the elucidation of the cation disorder, given the sensitivity for light nuclei such as Li [40].

Most experimental reports showed a significant capacity loss of AP-based cathodes during cycling. In addition to the structural considerations mentioned above, the choice of electrolyte might play an important role. For instance, sulfur leaching from active materials in conventional electrolytes (e.g. LP30) has indeed not been ruled out. Previous works on sulfides have studied several types of electrolytes (e.g. 1 M LiTFSI in DME:DOL 1:1 vol) to mitigate the migration of sulfur, which has not been done for AP cathodes. Thus, a systematic study of the stability of the electrode material in different electrolytes (which might also be inspired by Li-S batteries) upon cycling, as well as the CEI formation are still needed. This represents a perfect platform for the future design of the *operando* experiments to shine light at the interaction of the AP materials with the electrolytes. Thus, the tasks for the future *operando* characterization include not only elucidation of the electrochemical mechanism but also the influence of electrolytes on the operating mechanism.

3.3. Implications on modern battery landscape

There are two main niches that AP oxychalcogenides could be competitive in:

- The low-cost, geopolitically insensitive Li-ion market, taking advantage of the Fe-based archetypical composition, Li_2FeSO. This part of the market is currently led by LFP, and therefore further research should be done to make an adequate comparison. The two are comparable in terms of energy density since the lower voltage of the AP cathodes is compensated by its larger capacity as compared to LFP. The AP could have potential advantages with respect electronic conductivity (to be measured, lower bandgap predicted [50,51]), which could eliminate the need for carbon coating that is a

requirement for LFP and provide an opportunity to create fast -charging batteries.
- The current trends in the battery science highlight the importance of research towards solid-state batteries. In this context, the low and isotropic volume expansion could be hugely important, to alleviate the cracking and delamination phenomena that dominate capacity loss, and so dramatically increase cycle life. Furthermore, the low operating voltage (~2 V vs. Li/Li^+) could be beneficial to reduce oxidation of the electrolyte at the cathode and eliminate detrimental formation of resistive cathode electrolyte interphase (CEI). The sulfide nature of the cathode could potentially facilitate stable interfaces with the state-of-the-art sulfide solid electrolyte employed (e.g. the Li_6PS_5Cl argyrodite).

However, there are several directions to be highlighted to address the potential applicability of AP oxychalcogenides as cathode materials:

- further research is required to address the stability towards moisture. That property of oxychalcogenides restricts reliable preparation of A_2TMChO-based electrodes even at the laboratory scale, which possibly explains the discrepancies of the reported electrochemical results. Furthermore, a potential commercialization of oxychalcogenide materials could be achieved only if that problem can be mitigated.
- Low operating voltage of AP oxychalcogenide materials, even though it could be mitigated by the increased capacity, may represent a potential concern for some of the battery manufactures, which are primarily focused on the high-voltage cathodes for the next generation of batteries. Furthermore, the combination of high capacity and low voltage would necessitate a large amount of anode active material (e.g. graphite) to balance, potentially creating issues at the cell level. However, exploration of alternative compositions designed to improve operating voltage as covered in Section 3.1 could potentially address this problem.
- The participation of the chalcogenide ion in the electrochemical process —prerequisite to the high reported capacities — may potentially cause issues with the long-term cycling stability of AP oxychalcogenide materials.
- Development of Na-based analogues of AP could provide an alternative path towards commercial applicability of these materials.
- The unclear operation mechanism of AP oxychalcogenide materials calls for comprehensive *operando* studies, particularly in view of determination of the chalcogen participation in the electrochemical reactions.

4. Conclusions

Overall, the field of oxychalcogenide cathode materials represents an interesting playground with many possibilities for exploration of future materials and compounds: the chemical versatility provides such an opportunity. Further development and optimization of APs and ARPs could possibly allow these materials to challenge their main rival – LFP, which benefits from decades of development and optimization.

Funding

The PhD fellowship for T.D. was provided by the Department of Chemistry of University of Oslo. M.V. thanks the Norwegian Research Council (NFR) for their financial support through a project number 301711. M.W., X.K. and T.F. acknowledge the funding received from the Netherlands Organization for Scientific Research (NWO) under the VICI grant (no. 16122) and the open-competition XS grant (OCENW. XS22.4.210). T.F. acknowledges the funding provided by the European Union's HORIZON EUROPE program in the form of a Marie Skłodowska-Curie individual postdoctoral fellowship (project no. 101066486). X.K., T.F., M.R. and M.W. acknowledge the funding received from the ALISTORE ERI (CNRS 3104) in the form of the PhD fellowship for X.K. between T.U. Delft and CIC energiGUNE. A.Y.K. acknowledges the support of MoZEES, a Norwegian centre for Environment-friendly Energy Research (FME), co-sponsored by the Research Council of Norway (project number 257653). M.R. acknowledges the Spanish Ministerio de Industria, Comercio y Turismo and the European Union - Next Generation EU for their financial support through the project VEC-020100–2022–127/PP27.

CRediT authorship contribution statement

Tian Dai: Writing – review & editing, Writing – original draft, Visualization, Methodology, Formal analysis, Conceptualization. **Xavier Kouoi:** Writing – review & editing, Writing – original draft, Visualization, Methodology, Formal analysis, Conceptualization. **Marine Reynaud:** Writing – review & editing, Writing – original draft, Methodology, Conceptualization. **Marnix Wagemaker:** Supervision, Project administration. **Martin Valldor:** Writing – review & editing, Writing – original draft, Visualization, Supervision, Project administration, Methodology, Conceptualization. **Theodosios Famprikis:** Writing – review & editing, Writing – original draft, Visualization, Conceptualization. **Alexey Y. Koposov:** Writing – review & editing, Writing – original draft, Supervision, Project administration, Methodology, Conceptualization.

Declaration of competing interest

The authors declare that they have no known competing financial interests or personal relationships that could have appeared to influence the work reported in this paper.

References

[1] Z. Ogumi, R. Kostecki, D. Guyomard, M. Inaba, Lithium-Ion Batteries—the 25th anniversary of commercialization, Electrochem. Soc. Interface 25 (3) (2016) 65.
[2] M. Li, J. Lu, Z. Chen, K. Amine, 30 years of Lithium-Ion batteries, Adv. Mater. 30 (33) (2018) 1800561.
[3] M. Winter, B. Barnett, K. Xu, Before Li Ion batteries, Chem. Rev. 118 (23) (2018) 11433–11456.
[4] H. Chang, Y.-R. Wu, X. Han, T.-F. Yi, Recent developments in advanced anode materials for lithium-ion batteries, Energy Mater 1 (3) (2021) 24.
[5] G.G. Eshetu, H. Zhang, X. Judez, H. Adenusi, M. Armand, S. Passerini, E. Figgemeier, Production of high-energy Li-ion batteries comprising silicon-containing anodes and insertion-type cathodes, Nat. Commun. 12 (1) (2021) 5459.
[6] A. Manthiram, A reflection on lithium-ion battery cathode chemistry, Nat. Commun. 11 (1) (2020) 1550.
[7] K. Mizushima, P.C. Jones, P.J. Wiseman, J. Goodenough, LixCoO2 (0<x<-1): a new cathode material for batteries of high energy density, Mater. Res. Bull. 15 (1980) 783–789.
[8] W. Yao, M. Chouchane, W. Li, S. Bai, Z. Liu, L. Li, A.X. Chen, B. Sayahpour, R. Shimizu, G. Raghavendran, M.A. Schroeder, Y.-T. Chen, D.H.S. Tan, B. Sreenarayanan, C.K. Waters, A. Sichler, B. Gould, D.J. Kountz, D.J. Lipomi, M. Zhang, Y.S. Meng, A 5V-class cobalt-free battery cathode with high loading enabled by dry coating, Energy Environ. Sci. 16 (4) (2023) 1620–1630.
[9] A. Manthiram, J.B. Goodenough, Lithium-based polyanion oxide cathodes, Nature Energy 6 (8) (2021) 844–845.
[10] C. Masquelier, L. Croguennec, Polyanionic (phosphates, silicates, sulfates) frameworks as electrode materials for rechargeable Li (or Na) batteries, Chem. Rev. 113 (8) (2013) 6552–6591.
[11] F. Wu, G. Yushin, Conversion cathodes for rechargeable lithium and lithium-ion batteries, Energy Environ. Sci. 10 (2) (2017) 435–459.
[12] I. Hasa, S. Mariyappan, D. Saurel, P. Adelhelm, A.Y. Koposov, C. Masquelier, L. Croguennec, M. Casas-Cabanas, Challenges of today for Na-based batteries of the future: from materials to cell metrics, J. Power Sources 482 (2021) 228872.
[13] X. Wang, S. Roy, Q. Shi, Y. Li, Y. Zhao, J. Zhang, Progress in and application prospects of advanced and cost-effective iron (Fe)-based cathode materials for sodium-ion batteries, J. Mater. Chem. A 9 (4) (2021) 1938–1969.
[14] S. Comello, S. Reichelstein, The emergence of cost effective battery storage, Nat. Commun. 10 (1) (2019) 2038.
[15] E. Goikolea, V. Palomares, S. Wang, I.R. de Larramendi, X. Guo, G. Wang, T. Rojo, Na-ion batteries—approaching old and new challenges, Adv. Energy Mater. 10 (44) (2020) 2002055.
[16] K. Chayambuka, G. Mulder, D.L. Danilov, P.H.L. Notten, From Li-Ion batteries toward Na-Ion chemistries: challenges and opportunities, Adv. Energy Mater. 10 (38) (2020) 2001310.

[17] Y. Zhang, R. Zhang, Y. Huang, Air-Stable Na x TMO2 cathodes for sodium storage, Front. Chem. 7 (2019) 335.
[18] K. Liang, D. Wu, Y. Ren, X. Huang, J. Ma, Research progress on Na3V2 (PO4) 2F3-based cathode materials for sodium-ion batteries, Chin. Chem. Lett. 34 (6) (2023) 107978.
[19] J.W. Fergus, Recent developments in cathode materials for lithium ion batteries, J. Power Sources 195 (4) (2010) 939–954.
[20] M. Mohamed, M.V. Gorbunov, M. Valldor, S. Hampel, N. Gräßler, D. Mikhailova, Tuning the electrochemical properties by anionic substitution of Li-rich antiperovskite (Li 2 Fe) S 1− x Se x O cathodes for Li-ion batteries, J. Mater. Chem. A 9 (40) (2021) 23095–23105.
[21] Y. Lyu, X. Wu, K. Wang, Z. Feng, T. Cheng, Y. Liu, M. Wang, R. Chen, L. Xu, J. Zhou, An overview on the advances of LiCoO2 cathodes for lithium-ion batteries, Adv. Energy Mater. 11 (2) (2021) 2000982.
[22] C. Hendricks, N. Williard, S. Mathew, M. Pecht, A failure modes, mechanisms, and effects analysis (FMMEA) of lithium-ion batteries, J. Power Sources 297 (2015) 113–120.
[23] J. Lee, A. Urban, X. Li, D. Su, G. Hautier, G. Ceder, Unlocking the potential of Cation-disordered oxides for rechargeable lithium batteries, Science 343 (6170) (2014) 519–522.
[24] D.-H. Seo, J. Lee, A. Urban, R. Malik, S. Kang, G. Ceder, The structural and chemical origin of the oxygen redox activity in layered and cation-disordered Li-excess cathode materials, Nat. Chem. 8 (7) (2016) 692–697.
[25] A. Urban, A. Abdellahi, S. Dacek, N. Artrith, G. Ceder, Electronic-structure origin of cation disorder in transition-metal oxides, Phys. Rev. Lett. 119 (17) (2017) 176402.
[26] M.H. Braga, J.A. Ferreira, V. Stockhausen, J.E. Oliveira, A. El-Azab, Novel Li3ClO based glasses with superionic properties for lithium batteries, J. Mater. Chem. A 2 (15) (2014) 5470–5480.
[27] Z. Deng, D. Ni, D. Chen, Y. Bian, S. Li, Z. Wang, Y. Zhao, Anti-perovskite materials for energy storage batteries, InfoMat 4 (2) (2022) e12252.
[28] J.A. Dawson, T. Famprikis, K.E. Johnston, Anti-perovskites for solid-state batteries: recent developments, current challenges and future prospects, J. Mater. Chem. A 9 (35) (2021) 18746–18772.
[29] J. Zheng, B. Perry, Y. Wu, Antiperovskite superionic conductors: a critical review, ACS Mater. Au 1 (2) (2021) 92–106.
[30] J. Zhu, Y. Wang, S. Li, J.W. Howard, J. Neuefeind, Y. Ren, H. Wang, C. Liang, W. Yang, R. Zou, C. Jin, Y. Zhao, Sodium ion transport mechanisms in Antiperovskite electrolytes Na3OBr and Na4OI2: an in Situ neutron diffraction study, Inorg. Chem. 55 (12) (2016) 5993–5998.
[31] A.C. Coutinho Dutra, G.E. Rudman, K.E. Johnston, J.A. Dawson, Defect chemistry and ion transport in low-dimensional-networked Li-rich anti-perovskites as solid electrolytes for solid-state batteries, Energy Adv. 2 (5) (2023) 653–666.
[32] K.T. Lai, I. Antonyshyn, Y. Prots, M. Valldor, Anti-Perovskite Li-battery cathode materials, J. Am. Chem. Soc. 139 (28) (2017) 9645–9649.
[33] K.T. Lai, I. Antonyshyn, Y. Prots, M. Valldor, Extended chemical flexibility of cubic Anti-Perovskite lithium battery cathode materials, Inorg. Chem. 57 (21) (2018) 13296–13299.
[34] M. Valldor, T. Wright, A. Fitch, Y. Prots, Metal vacancy ordering in an Antiperovskite resulting in two modifications of Fe2SeO, Angew. Chem. Int. Ed. 55 (32) (2016) 9380–9383.
[35] D. Mikhailova, L. Giebeler, S. Maletti, S. Oswald, A. Sarapulova, S. Indris, Z. Hu, J. Bednarcik, M. Valldor, Operando studies of antiperovskite lithium battery cathode material (Li2Fe)SO, ACS Appl. Energy Mater. 1 (11) (2018) 6593–6599.
[36] A. Urban, I. Matts, A. Abdellahi, G. Ceder, Computational design and preparation of cation-disordered oxides for high-energy-density Li-ion batteries, Adv. Energy Mater. 6 (15) (2016) 1600488.
[37] M.M. Thackeray, W.I.F. David, P.G. Bruce, J.B. Goodenough, Lithium insertion into manganese spinels, Mater. Res. Bull. 18 (4) (1983) 461–472.
[38] L. Gao, X. Zhang, J. Zhu, S. Han, H. Zhang, L. Wang, R. Zhao, S. Gao, S. Li, Y. Wang, D. Huang, Y. Zhao, R. Zou, Boosting lithium ion conductivity of antiperovskite solid electrolyte by potassium ions substitution for cation clusters, Nat. Commun. 14 (1) (2023) 6807.
[39] L. Gao, M. Song, R. Zhao, S. Han, J. Zhu, W. Xia, J. Bian, L. Wang, S. Gao, Y. Wang, R. Zou, Y. Zhao, Effects of fluorination on crystal structure and electrochemical performance of antiperovskite solid electrolytes, J. Energy Chem. 77 (2023) 521–528.
[40] L. Gao, J. Pan, L. Di, J. Zhu, L. Wang, S. Gao, R. Zou, L. Kang, S. Han, Y. Zhao, Neutron diffraction for revealing the structures and ionic transport mechanisms of antiperovskite solid electrolytes, Chinese J. Struct. Chem. 42 (5) (2023) 100048.
[41] Y. Yu, Z. Wang, G. Shao, Theoretical tuning of Ruddlesden–Popper type anti-perovskite phases as superb ion conductors and cathodes for solid sodium ion batteries, J. Mater. Chem. A 7 (17) (2019) 10483–10493.
[42] S.-J. Song, J.-Y. Lu, Q.-Q. Zhu, Z. Ren, G.-H. Cao, Crystal structure and physical properties of layered Na2Fe2S2O, J. Phys. Chem. Solids 181 (2023) 111469.
[43] J. Gamon, A.J. Perez, L.A. Jones, M. Zanella, L.M. Daniels, R.E. Morris, C.C. Tang, T.D. Veal, L.J. Hardwick, M.S. Dyer, Na 2 Fe 2 OS 2, a new earth abundant oxysulphide cathode material for Na-ion batteries, J. Mater. Chem. A 8 (39) (2020) 20553–20569.
[44] M.V. Gorbunov, T. Doert, D. Mikhailova, Na2Fe2Se2O: a double anti-perovskite with prevalence of anionic redox activity in Na-ion batteries, Chem. Commun. 59 (92) (2023) 13763–13766.
[45] K. Momma, F. Izumi, VESTA 3 for three-dimensional visualization of crystal, volumetric and morphology data, J. Appl. Crystallogr. 44 (6) (2011) 1272–1276.
[46] A. Simonov, A.L. Goodwin, Designing disorder into crystalline materials, Nature Rev. Chem. 4 (12) (2020) 657–673.
[47] M. Reynaud, J. Serrano-Sevillano, M. Casas-Cabanas, Imperfect battery materials: a closer look at the role of defects in electrochemical performance, Chem. Mater. 35 (9) (2023) 3345–3363.
[48] S.W. Coles, V. Falkowski, H.S. Geddes, G.E. Pérez, S.G. Booth, A.G. Squires, C. O'Rourke, K. McColl, A.L. Goodwin, S.A. Cussen, S.J. Clarke, M.S. Islam, B. J. Morgan, Anion-polarisation-directed short-range-order in antiperovskite Li2FeSO, J. Mater. Chem. A 11 (24) (2023) 13016–13026.
[49] Z. Deng, D. Chen, M. Ou, Y. Zhang, J. Xu, D. Ni, Z. Ji, J. Han, Y. Sun, S. Li, Cation disordered anti-perovskite cathode materials with enhanced lithium diffusion and suppressed phase transition, Adv. Energy Mater. 13 (28) (2023) 2300695.
[50] Z. Lu, F. Ciucci, Anti-perovskite cathodes for lithium batteries, J. Mater. Chem. A 6 (12) (2018) 5185–5192.
[51] B. Zhu, D.O. Scanlon, Predicting lithium iron Oxysulfides for battery cathodes, ACS Appl. Energy Mater. 5 (1) (2022) 575–584.
[52] R. Zhang, S. Yang, H. Li, T. Zhai, H. Li, Air sensitivity of electrode materials in Li/Na ion batteries: issues and strategies, InfoMat 4 (6) (2022) e12305.
[53] M.V. Gorbunov, S. Carrocci, S. Maletti, M. Valldor, T. Doert, S. Hampel, I. G. Gonzalez Martinez, D. Mikhailova, N. Gräßler, Synthesis of (Li2Fe1–y Mn SO Antiperovskites with comprehensive investigations of (Li2Fe0. 5Mn0. 5) SO as cathode in Li-ion batteries, Inorg. Chem. 59 (21) (2020) 15626–15635.
[54] M.V. Gorbunov, S. Carocci, I.G. Gonzalez Martinez, V. Baran, D. Mikhailova, Studies of Li2Fe0. 9M0. 1SO Antiperovskite materials for lithium–ion batteries: the role of partial Fe2+ to M2+ substitution, Front. Energy Res. 9 (2021) 657962.
[55] M. Miura, K. Hikima, A. Matsuda, Fabrication and electrochemical characterization of an all-solid-state battery with an Anti-perovskite electrode material (Li2Fe)SO, Chem. Lett. 51 (7) (2022) 690–692.
[56] M.A.A. Mohamed, L. Singer, H. Hahn, D. Djendjur, A. Özkara, E. Thauer, I. G. Gonzalez-Martinez, M. Hantusch, B. Büchner, S. Hampel, R. Klingeler, N. Gräßler, Lithium-rich antiperovskite (Li2Fe)SeO: a high-performance cathode material for lithium-ion batteries, J. Power Sources 558 (2023) 232547.
[57] T. Tsuzuki, P.G. McCormick, Mechanochemical synthesis of nanoparticles, J. Mater. Sci. 39 (16) (2004) 5143–5146.
[58] E. Ahiavi, J.A. Dawson, U. Kudu, M. Courty, M.S. Islam, O. Clemens, C. Masquelier, T. Famprikis, Mechanochemical synthesis and ion transport properties of Na3OX (X = Cl, Br, I and BH4) antiperovskite solid electrolytes, J. Power Sources 471 (2020) 228489.
[59] P. Baláž, M. Hegedüs, M. Achimovičová, M. Baláž, M. Tešinský, E. Dutková, M. Kaňuchová, J. Briančin, Semi-industrial green mechanochemical syntheses of solar cell absorbers based on quaternary sulfides, ACS Sustain. Chem. Eng 6 (2018) 2132–2141.
[60] M.A.A. Mohamed, H.A.A. Saadallah, I.G. Gonzalez-Martinez, M. Hantusch, M. Valldor, B. Büchner, S. Hampel, N. Gräßler, Mechanochemical synthesis of Li-rich (Li2Fe)SO cathode for Li-ion batteries, Green Chem. 25 (10) (2023) 3878–3887.
[61] L. Singer, M.A.A. Mohamed, H. Hahn, I.G. Gonzalez-Martinez, M. Hantusch, K. Wenelska, E. Mijowska, B. Büchner, S. Hampel, N. Gräßler, R. Klingeler, Elucidating the electrochemical reaction mechanism of lithium-rich antiperovskite cathodes for lithium-ion batteries as exemplified by (Li2Fe)SeO, J. Mater. Chem. A 11 (26) (2023) 14294–14303.
[62] M. Miura, K. Hikima, A. Matsuda, Fabrication and electrochemical characterization of an all-solid-state battery with an Anti-perovskite electrode material (Li2Fe) SO, Chem. Lett. 51 (7) (2022) 690–692.
[63] T.K. Schwietert, A. Vasileiadis, M. Wagemaker, First-principles prediction of the electrochemical stability and reaction mechanisms of solid-state electrolytes, JACS Au 1 (9) (2021) 1488–1496.
[64] M. Osiak, H. Geaney, E. Armstrong, C. O'Dwyer, Structuring materials for lithium-ion batteries: advancements in nanomaterial structure, composition, and defined assembly on cell performance, J. Mater. Chem. A 2 (25) (2014) 9433–9460.
[65] V.M. Goldschmidt, Die gesetze der krystallochemie, Naturwissenschaften 14 (21) (1926) 477–485.
[66] R.D. Shannon, Revised effective ionic radii and systematic studies of interatomic distances in halides and chalcogenides, Acta Crystallographica Sect. A: Cryst. Phys. Diffract. Theor. General Crystallogr. 32 (5) (1976) 751–767.
[67] http://abulafia.mt.ic.ac.uk/shannon/ptable.php.
[68] D.A. Keen, A.L. Goodwin, The crystallography of correlated disorder, Nature 521 (7552) (2015) 303–309.
[69] C. Röhr, Crystal structure of calcium germanide oxide, Ca3GeO, Zeitschrift für Kristallographie-Crystalline Mater. 210 (10) (1995) 781. -781.
[70] A. Widera, H. Schäfer, Übergangsformen zwischen zintlphasen und echten salzen: die verbindungen A3BO (MIT A=Ca, Sr, Ba und B=Sn, Pb), Mater. Res. Bull. 15 (12) (1980) 1805–1809.
[71] D. Han, M.-H. Du, M. Huang, S. Wang, G. Tang, T. Bein, H. Ebert, Ground-state structures, electronic structure, transport properties and optical properties of Ca-based anti-Ruddlesden-Popper phase oxide perovskites, Phys. Rev. Mater. 6 (11) (2022) 114601.